Cherenkov radiation and scattering of external dispersive waves by two-color solitons

Ivan Oreshnikov,[1,*] Oliver Melchert,[2,3,4] Stephanie Willms,[2,3] Surajit Bose,[3] Ihar Babushkin,[2,3] Ayhan Demircan,[2,3,4] and Alexey Yulin[5]

[1] *Max Planck Institute for Intelligent Systems, Max-Planck-Ring 4, 72076 Tübingen, Germany*
[2] *Cluster of Exellence PhoenixD, Welfengarten 1, 30167 Hannover, Germany*
[3] *Institute of Quantum Optics, Leibniz Universität Hannover, Welfengarten 1, 30167 Hannover, Germany*
[4] *Hannover Centre for Optical Technologies, Neinburger Strasse 17, 30167 Hannover, Germany*
[5] *Department of Nanophotonics and Metamaterials, ITMO University, Kronverskiy pr. 49, 19701 St. Petersburg, Russia*

(Dated: April 24, 2022)

In dispersion landscapes with two separate regions of anomalous dispersion it is possible to create a quasi-stable two-color solitary wave. In this paper we consider how those waves interact with dispersive radiation, including the processes of Cherenkov radiation generation as well as the processes of external wave scattering. We derive the analytic resonance conditions and verify them through numeric experiments. We also report incident radiation driving the internal oscillations of the soliton during the scattering process in case of a more intensive incident radiation. We generalize the resonance conditions for the case of an oscillating soliton and demonstrate how one can use scattering process to probe the internal mode.

INTRODUCTION

From the prior work [1] we know that if the dispersion landscape $\beta(\omega)$ has two regions of anomalous dispersion separated by a region of normal dispersion, it is possible to create a quasi-stable configuration of two tightly-coupled solitons each propagating on its own carrier frequency. This coupled state, especially in the process of initial evolution, sheds dispersive waves that resembles Cherenkov radiation that is observed for other types of solitary waves in vast variety of settings [2–7].

Nullam eu ante vel est convallis dignissim. Fusce suscipit, wisi nec facilisis facilisis, est dui fermentum leo, quis tempor ligula erat quis odio. Nunc porta vulputate tellus. Nunc rutrum turpis sed pede. Sed bibendum. Aliquam posuere. Nunc aliquet, augue nec adipiscing interdum, lacus tellus malesuada massa, quis varius mi purus non odio. Pellentesque condimentum, magna ut suscipit hendrerit, ipsum augue ornare nulla, non luctus diam neque sit amet urna. Curabitur vulputate vestibulum lorem. Fusce sagittis, libero non molestie mollis, magna orci ultrices dolor, at vulputate neque nulla lacinia eros. Sed id ligula quis est convallis tempor. Curabitur lacinia pulvinar nibh. Nam a sapien.

Pellentesque dapibus suscipit ligula. Donec posuere augue in quam. Etiam vel tortor sodales tellus ultricies commodo. Suspendisse potenti. Aenean in sem ac leo mollis blandit. Donec neque quam, dignissim in, mollis nec, sagittis eu, wisi. Phasellus lacus. Etiam laoreet quam sed arcu. Phasellus at dui in ligula mollis ultricies. Integer placerat tristique nisl. Praesent augue. Fusce commodo. Vestibulum convallis, lorem a tempus semper, dui dui euismod elit, vitae placerat urna tortor vitae lacus. Nullam libero mauris, consequat quis, varius et, dictum id, arcu. Mauris mollis tincidunt felis. Aliquam feugiat tellus ut neque. Nulla facilisis, risus a rhoncus fermentum, tellus tellus lacinia purus, et dictum nunc justo sit amet elit.

ANALYTIC MODEL

In this section we derive a perturbation theory that explains the resonance conditions that were proposed before in [1], demonstrate additional Cherenkov radiation mechanisms due to four-wave mixing between the frequency components of the soliton, and then we extend this theory to describe the process of external waves scattering on the soliton.

We start by considering a non-envelope version of a nonlinear Schrödinger equation [8]

$$i\partial_z\tilde{u} + \beta(\omega)\tilde{u}(z,\omega) + \gamma(\omega)\mathcal{F}\left\{|u|^2 u(z,t)\right\}_{(\omega>0)} = 0. \quad (1)$$

Here and further tilde indicates a Fourier image of the field and $\mathcal{F}\{\cdots\}_{(\omega>0)}$ is the explicit Fourier transform over the positive frequencies.

To build the perturbation theory let us introduce an ansatz that represents the solution as a sum of two single-frequency solitary waves $U_{1,2}(z,t)$ and a small residue radiation $\psi(z,t)$

$$u(z,t) = U_1(z,t) + U_2(z,t) + \psi(z,t) \quad (2)$$
$$|\psi| \ll |U_1| \sim |U_2|\,.$$

For the solitary waves $U_{1,2}(z,t)$ we assume that they satisfy a pair of coupled nonlinear Schrödinger equations below

$$i\partial_z U_n + \beta_n(i\partial_t)U_n(z,t) + \gamma(\omega_n)\left(|U_n|^2 U_n + 2\,|U_m|^2 U_n\right) = 0, \tag{3}$$

where $n = 1, 2$ and $m = 2, 1 \neq n$. Essentially, this is an assumption that the solitons are coupled strictly by inducing a refractive-index potential on each other [9], and each soliton exists in some sort of a truncated dispersion landscape that is defined by the operator $\beta_n(i\partial_t)$. A reasonable guess for a truncated operator is a parabolic approximation close to the carrier frequency

$$\beta_n(i\partial_t) = \beta(\omega_n) + i\beta'(\omega_n)\partial_t - \frac{1}{2}\,\beta''(\omega_n)\partial_t^2 \tag{4}$$

We additionally propose that in the soliton's frame of reference the envelope evolves with wavenumber $k_n(\omega)$ which we approximate by the wavenumber of the fundamental soliton in the ordinary nonlinear Schrödinger equation and a correction from a secondary soliton as

$$k_n(\omega) \approx \frac{\gamma(\omega_n)A_n^2}{2} + \beta(\omega_n) + \beta'(\omega_n)(\omega - \omega_n) + \gamma(\omega_n)A_m^2 \tag{5}$$

where $n = 1, 2$, $m = 2, 1 \neq n$ and A_n is the soliton amplitude.

By substituting ansatz (2) into equation (1), linearizing with respect to perturbation $\psi(z,\omega)$, and discarding the terms corresponding to the soliton equations (3) we get the equation for $\tilde{\psi}$

$$\begin{aligned} i\partial_z\tilde{\psi} + \beta(\omega)\tilde{\psi}(z,\omega) + \gamma(\omega)\mathcal{F}\left\{2\,|U_1+U_2|^2\,\psi + (U_1+U_2)^2\,\psi^*\right\}_{(\omega>0)} = \\ -\left[\beta(\omega)-\beta_1(\omega)\right]\tilde{U}_1(z,\omega) - \left[\beta(\omega)-\beta_2(\omega)\right]\tilde{U}_2(z,\omega) - \gamma(\omega)\mathcal{F}\left\{U_2^2U_1^* + U_1^2U_2^*\right\}_{(\omega>0)} \end{aligned} \tag{6}$$

In the right-hand's side of equation (6) we see two types of driving terms and each of those terms can be in resonance with the linear dispersive waves that exist in the system, if the particular wavenumber $k(\omega_*)$ of the driving term is equal to a wavenumber of a dispersive wave $\beta(\omega_*)$ at some frequency ω_* [2, 10]. The first type of the terms is $[\beta(\omega) - \beta_n(\omega)]\,\tilde{U}_n(z,\omega)$ which drives the generation of Cherenkov radiation by an individual soliton U_n if the following resonance condition is satisfied

$$\beta(\omega) = k_n(\omega). \tag{7}$$

The second type of the terms are $\gamma(\omega)\mathcal{F}\left\{U_2^2U_1^*\right\}$ and $\gamma(\omega)\mathcal{F}\left\{U_1^2U_2^*\right\}$ and they correspond to the process of four-wave mixing that in our case results in generation of dispersive radiation at some frequency where

$$\beta(\omega) = 2k_n(\omega) - k_m(\omega). \tag{8}$$

Let us move on to the problem of external dispersive wave scattering. For that we split the perturbation into the incident and the scattered parts

$$\psi(z,t) = \psi_{\text{inc}}(z,t) + \psi_{\text{sc}}(z,t). \tag{9}$$

We explicitly define $\psi_{\text{inc}}(z,t)$ as a linear wave that is propagating in a soliton-free medium

$$i\partial_z\tilde{\psi}_{\text{inc}}(z,t) + \beta(\omega)\tilde{\psi}_{\text{inc}}(z,t) = 0. \tag{10}$$

Substituting equation (9) into (6) and eliminating the terms corresponding to (10) we are left with equation for the scattered component

$$\begin{aligned} i\partial_z\tilde{\psi}_{\text{sc}} + \beta(\omega)\tilde{\psi}_{\text{sc}}(z,\omega) + \gamma(\omega)\mathcal{F}\left\{2\,|U_1+U_2|^2\,\psi_{\text{sc}} + (U_1+U_2)^2\,\psi_{\text{sc}}^*\right\}_{(\omega>0)} = \ldots\,\text{(omitted is the RHS from (6))} \\ -\gamma(\omega)\mathcal{F}\left\{2\left(|U_1|^2 + U_1U_2^* + U_2U_1^* + |U_2|^2\right)\psi_{\text{inc}} + \left(U_1^2 + 2\,U_1U_2 + U_2^2\right)\psi_{\text{inc}}^*\right\}_{(\omega>0)} \end{aligned} \tag{11}$$

In addition to the resonance terms already discussed in equation (6) we see the terms that arise due to interaction

between the incident radiation and the soliton. In here six new types of resonance behaviour are possible. The first one is due to terms $|U_1|^2\psi_{\rm inc}$ and $|U_2|^2\psi_{\rm inc}$, both with the resonance condition

$$\beta(\omega_{\rm sc}) = \beta(\omega_{\rm inc}) \tag{12}$$

The next two are due to mixed terms $U_1U_2^*\psi_{\rm inc}$ and $U_2U_1^*\psi_{\rm inc}$, with the corresponding resonance condition being

$$\beta(\omega_{\rm sc}) = \pm k_1 \mp k_2 + \beta(\omega_{\rm inc}) \tag{13}$$

Another two are due to $U_n^2\psi_{\rm inc}^*$ and the resonance condition is

$$\beta(\omega_{\rm sc}) = 2k_n(\omega_{\rm sc}) - \beta(\omega_{\rm inc}),\ n = 1, 2. \tag{14}$$

The final one is due to $2U_1U_2\psi_{\rm inc}^*$ with the resonances at

$$\beta(\omega_{\rm sc}) = k_1(\omega_{\rm sc}) + k_2(\omega_{\rm sc}) - \beta(\omega_{\rm inc}). \tag{15}$$

To verify the predictions given by resonance conditions (7), (8), (12), (13), (14), and (15) we proceed to numeric experiments.

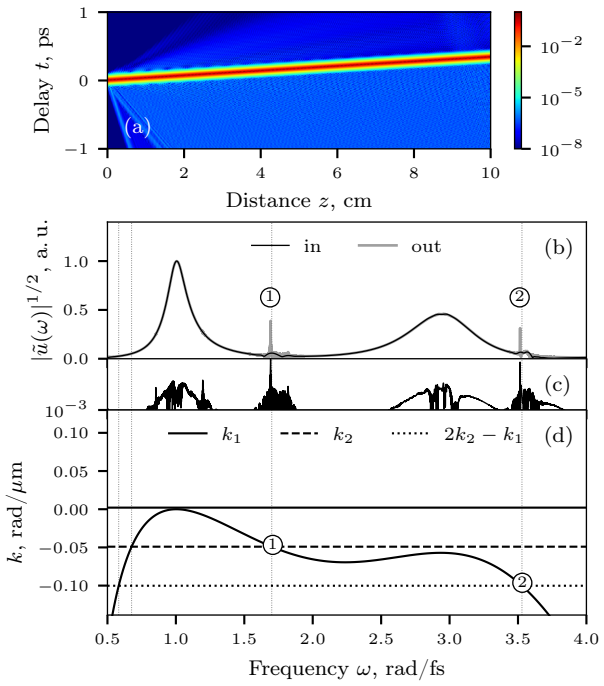

FIG. 1: (color online) Cherenkov radiation of an isolated soliton produced by the soliton with $\omega_1 = 1.010$ rad/fs. (a) time-domain view, (b) input and output spectra (c) spectra difference in log scale, and (d) resonance conditions diagram.

NUMERIC EXPERIMENTS

To numerically integrate equation (1) we use the integrating factor method and transform the equation into a non-stiff version for a modified spectrum [11]. The modified equation can be handled by any standard ODE solver; we use a `scipy` interface to `ZVODE` solver from `ODEPACK` [12, 13] (the simulation and the plotting code used in the paper can be found in [14]).

To study Cherenkov radiation of two color solitons we chain two separate simulations. First, following the prior work [1], we produce a two-color soliton by integrating an initial condition that is given by a sum of two fundamental solitons of standard NLSE

$$u_0(t) = A_1\,\mathrm{sech}(t/T_1)e^{-i\omega_1 t} + A_2\,\mathrm{sech}(t/T_2)e^{-i\omega_2 t}, \tag{16}$$

where frequency ω_1 is an arbitrary parameter (the only requirement is that it lies in the region of anomalous dispersion) and frequency ω_2 is chosen such that group velocities of both the frequency components match

$$\beta'(\omega_1) = \beta'(\omega_2).$$

In most of the simulations in this paper we fix $T_1 = T_2 = 20$ fs and the amplitudes A_1 and A_2 are chosen as the fundamental soliton amplitudes at the corresponding frequencies. This configuration sheds significant amount of radiation and relaxes to a quasi-stable solitary wave. We run the simulation until we reach $z = 10$ cm and then we take the output field of this seed simulation and suppress the radiation tails by multiplying it by a super-Gaussian window centered around the soliton peak. This isolated soliton serves as an input to the second simulation that is carried with the same parameters as the original one.

Once we suppress the initial radiation that is shed by the seed soliton during the relaxation process, the isolated soliton propagates generating only a narrow-spectrum Cherenkov radiation. As an example we can consider Fig. 1. Panel Fig. 1b shows normalized spectral densities at the input and the output of the simulation. The difference in spectra between the input and the output can be also seen in a logarithmic scale in panel Fig. 1c. There one can notice that on top of the input spectrum (plotted in Fig. 1b by thin black line) arise two additional spectral lines in the output spectrum (plotted by thicker gray line). Panel Fig. 2d demonstrates resonance conditions (7) and (8): black curve corresponds to the left-hand's side of both equations $\beta(\omega)$, horizontal lines correspond to the right-hand's sides. Intersections between the dispersive curve and the horizontal lines that contribute to Cherenkov radiation are marked separately: ① is the radiation due to the second component of the soliton as predicted by equation (7), ② is due to FWM between the frequency components that results in a radiation corresponding to wavenumber $2k_2 - k_1$, as predicted by (8).

To study the scattering processes we perform the seed

simulation and isolate the soliton. To that we add an incident dispersive wave in the form of a Gaussian pulse

$$\psi_{inc}(t) = A_{\text{inc}} \exp\left(-\frac{(t-t_0)^2}{T_{\text{inc}}^2} - i\omega_{\text{inc}} t\right).$$

In this section we pick A_{inc} as 1% of the maximum amplitude of the isolated soliton and fix the width to 300 fs. Central location t_0 is chosen as ± 1000 fs from the soliton center — the sign depends on the relative group velocity between the soliton and the dispersive wave. In the process of evolution the incident radiation interacts with the soliton to produce scattered radiation. This process can evolve in several different ways depending on the frequencies of the soliton and the incident radiation. In here we consider three concrete examples. In each of them the incident radiation is split between three different components.

The first configuration is very close to the degenerate case where the wavenumbers of the individual soliton components k_1 and k_2 coincide. Equation (13) then turns into equation (12). This case resembles the case of fundamental single-component soliton [10], however, due to shape of the dispersive curve $\beta(\omega)$ there is now more than one nontrivial solution to equation (12) and a single incident frequency corresponds up to four possible resonances. This configuration can be seen in Fig. 2. In practice, only some of them actually contribute to the scattered radiation. Again, those solution are separately marked on a diagram on panel 2d: ⓘ corresponds both to the incident and the partially transmitted radiation, ① is the reflected component and ② is the additional transmitted component.

The second configuration (seen in Fig. 3) is a case with significant difference between k_1 and k_2. Since (13) is no longer degenerate, the resonance diagram in Fig. 3d is more complex. However, as one can notice, in that case only solution marked with ② , corresponding to the upper (i.e. "$-,+$") branch of (13), contributes to the scattered radiation. Component ① , corresponding to the scattered radiation, comes from (12). The unmarked spectral line close to $\omega \approx 2.4$ is the Cherenkov radiation of the soliton itself.

The third configuration (seen in Fig. 4) is, in a sense, symmetric to the previous case. In here, again, the difference between k_1 and k_2 is significant and equation (13) is far from being degenerate, but in this case the resonances from the lower (i.e. "$+,-$") branch of (13) play a significant role. This is achieved by choosing the incident frequency greater than the carrier frequency of the second soliton component and enhanced by using an asymmetric seed soliton with $T_1 = 30$ fs and $T_2 = 10$ fs. This creates a solitary wave with the amplitude of the second component almost equal to the ampltiude of the first one.

Overall, in all of our experiments, only the scattered components corresponding to equations (12) and (13) turn out to be significant, while the components predicted by (14) and (15) do not seem to contribute to the resulting radiation. In other words, the terms proportional to $\tilde{\psi}^*_{inc}$ in the right hand's side of equation (11) can be safely neglected.

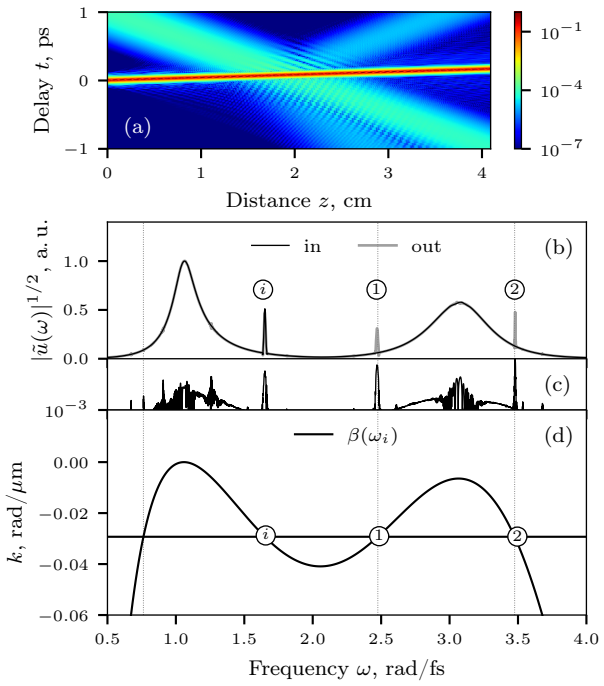

FIG. 2: (color online) Scattering of a weak DW with carrier frequency $\omega_{\text{inc}} = 1.650$ rad/fs on a soliton with first-component carrier frequency $\omega_1 = 1.070$ rad/fs. (a) time-domain view, (b) input and output spectra (c) spectra difference in log scale, and (d) resonance conditions diagram.

NONLINEAR EFFECTS

When deriving the resonance conditions (12) – (15) we assumed that the parameters of the solitons themselves stay constant throughout propagation and scattering processes. This can be considered a reasonable approximation when the ampltiude of the incident wave is negligible compared to the ampltidues of the individual soliton components. However, in the general case of a more intensive incident radiation this assumption does not hold. In this section we will briefly discuss two specific examples, where during scattering the interaction with the incident dispersive wave changes the parameters of the soliton. General setup of the experiments stay the same — we consider scattering of a Gaussian pulse on an isolated two-color soliton — but this time we pick DW ampltiude to be equal to 5% of the soliton's maximum amplitude. This change might seem subtle, but this is sufficient to make the scattering dynamics much more interesting.

In the first example (displayed in Figure 5) we consider

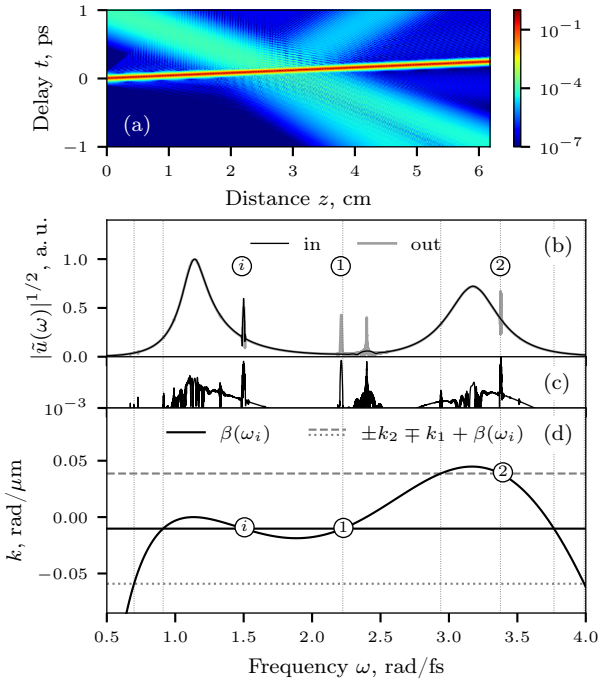

FIG. 3: (color online) Scattering of a weak DW with carrier frequency $\omega_{\text{inc}} = 1.500$ rad/fs on a soliton with first-component carrier frequency $\omega_1 = 1.150$ rad/fs. (a) time-domain view, (b) input and output spectra (c) spectra difference in log scale, and (d) resonance conditions diagram.

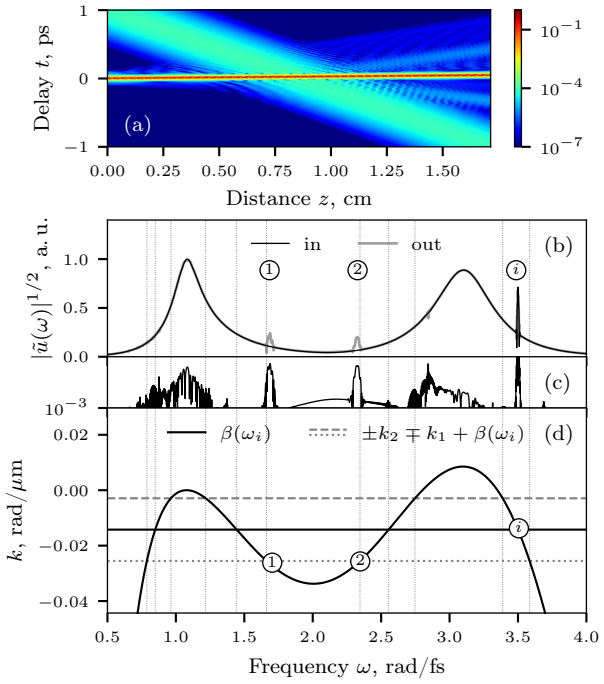

FIG. 4: (color online) Scattering of a weak DW with carrier frequency $\omega_{\text{inc}} = 3.500$ rad/fs on a soliton with first-component carrier frequency $\omega_1 = 1.085$ rad/fs. (a) time-domain view, (b) input and output spectra (c) spectra difference in log scale, and (d) resonance conditions diagram.

scattering of a dispersive wave with the incident frequency $\omega_i = 2.100$ rad/fs on a soliton with $\omega_1 = 1.010$ rad/fs. We see that an intensive dispersive wave can pull the soliton during scattering. This effect has been demonstrated before for the classical bright solitons of nonlinear Schrödinger equation [15, 16]. What is remarkable about this interaction in case of a two-color soliton is the fact that the soliton appears to be stable during this process. Granted, the frequency offset gained by the soliton during the scattering is not especially prominent (panel 5b.2), but at the same time the amplitude difference in both the frequency components stays under 1% (panel 5b.1), so almost no power loss occurs.

In the second example (displayed in Figure 6) we consider scattering of a dispersive wave with the incident frequency $\omega_i = 1.100$ rad/fs on a soliton with $\omega_1 = 1.010$ rad/fs. As it is evident from the soliton parameters displayed in panels 6b.1 and 6b.2, the incident radiation pumps an internal mode of the soliton during the scattering; the period of those oscillations can be estimated as $Z_0 = 2$ mm. The interaction of oscillating nonlinear waves, both the radiation and the scattering processes, is a well studied problem [4–7, 17] and the common trait in this setting, independent on the nature of the soliton oscillations, is that the dispersive radiation produced (generated or scattered) by the soliton is polychromatic, i.e. it consists of several isolated spectral components. This is indeed what we see in the output spectrum on panel 6c. To explain this behavior let us return to equations (6) and (11). In the oscillating case the individual solitons U_1 and U_2 are no longer represented by a single spatial frequency $\propto e^{ik_1 z}$ and $\propto e^{ik_2 z}$, but instead each of them corresponds to a Fourier series

$$U_n(z,t) = \sum_{N\in\mathbb{Z}} C_n(t) \exp\left(ik_1 z + i\frac{2\pi N}{Z_0} z \right),$$

where Z_0 is the oscillation period. This leads to a split in resonance conditions, and for the oscillating case equations (7), (8), (12) and (13) should read

$$\beta(\omega) = k_n(\omega) + \frac{2\pi N}{Z_0} \qquad (7^*)$$

$$\beta(\omega) = 2k_n(\omega) - k_m(\omega) + \frac{2\pi N}{Z_0} \qquad (8^*)$$

$$\beta(\omega_{\text{sc}}) = \beta(\omega_{\text{inc}}) + \frac{2\pi N}{Z_0} \qquad (12^*)$$

$$\beta(\omega_{\text{sc}}) = \pm k_1 \mp k_2 + \beta(\omega_{\text{inc}}) + \frac{2\pi N}{Z_0}, \qquad (13^*)$$

here $N \in \mathbb{Z}$ selects the harmonic.

The resonance conditions for the scattering process in the last simulation displayed on panel 6d. In this process only the last two equations (12) and (13) are relevant. The solid black lines correspond to equation (12) with

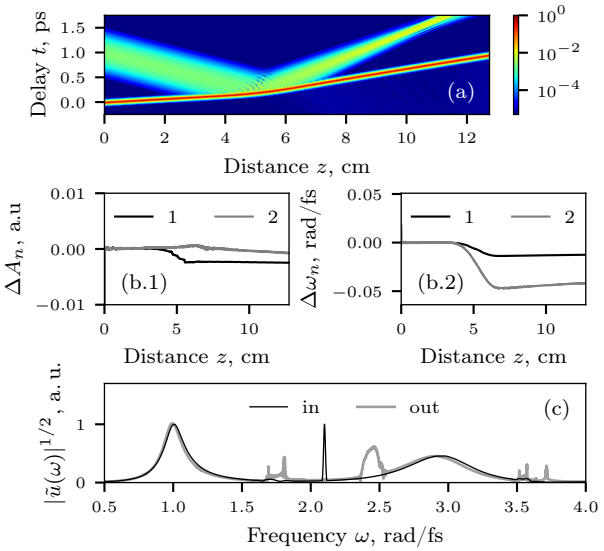

FIG. 5: (color online) Scattering of an intensive DW with carrier frequency $\omega_{\text{inc}} = 2.100$ rad/fs on a soliton with first-component carrier frequency $\omega_1 = 1.010$ rad/fs. (a) time-domain view (b.1, 2) soliton amplitude and central frequency oscillations (c) output spectrum.

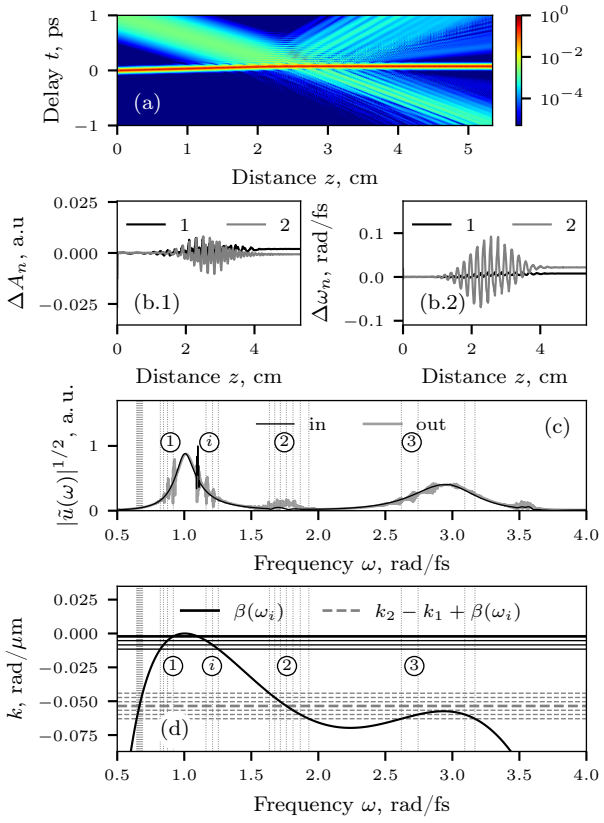

FIG. 6: (color online) Scattering of an intensive DW with carrier frequency $\omega_{\text{inc}} = 1.100$ rad/fs on a soliton with first-component carrier frequency $\omega_1 = 1.010$ rad/fs. (a) time-domain view (b.1, 2) soliton amplitude and central frequency oscillations (c) output spectrum (d) resonance condition diagram.

harmonics $N = -3, \ldots, 0$. This harmonic split leads not only to the reflected part of the radiation ① becoming polychromatic, but also has the same effect on the incident component ⓘ . Resonance condition (13) is represented by the gray dashed lines for harmonics $N = -3, \ldots, +3$. It contributes to the scattered radiation twice: with a wide band ② that otherwise would degenerate into a sharp spectral line in a non-oscillating case, and with three wide spectral lines in vicinity of ③ which is the contribution of the lower harmonics $N = -3, -2, -1$. One can notice that there is only two vertical lines corresponding to the numeric solution of (13) displayed around ③ . This is merely due to a small numeric error in estimating the soliton wavenumber k_2 in the plotting procedure, which causes harmonic $N = -1$ to touch the dispersive rather than intersect it.

The specific oscillation mode we see in Fig. 6 appears to be heavily damped, since launching the initial soliton with an additional frequency detuning does not lead to free frequency oscillations during propagation. However, since the incident radiation acts as a forcing element in this oscillator, one could expect to see some sort of a resonance behavior in here as well. And indeed, by adjusting the incident radiation frequency ω_i one can affect, to a certain degree, the amplitude of frequency oscillations of the second component ω_2. Panel Fig. 7a displays the dependency between $\Delta\omega_2$ during oscillations as a function of the incident frequency and indeend one can notice a typical resonance curve. For this specific mode, where the frequency oscillations dominate, it is relatively straightforward to get an estimate for the period Z_0 of the mode and the corresponding wavenumber K_0 (see Supplementary for the concrete results). When one superimposes this resonance wavenumber K_0 over the dispersive curve as it is shown in Fig. 7b, one can estimate the resonance incident frequency corresponding to this internal resonance. Vertical dashed line in both Fig. 7a and Fig. 7b marks this resonance frequency and from the resonance curve above we can confirm that indeed our estimates are correct.

CONCLUSION

Pellentesque dapibus suscipit ligula. Donec posuere augue in quam. Etiam vel tortor sodales tellus ultricies commodo. Suspendisse potenti. Aenean in sem ac leo mollis blandit. Donec neque quam, dignissim in, mollis nec, sagittis eu, wisi. Phasellus lacus. Etiam laoreet quam sed arcu. Phasellus at dui in ligula mollis ultricies. Integer placerat tristique nisl. Praesent augue. Fusce commodo. Vestibulum convallis, lorem a tempus semper, dui dui euismod elit, vitae placerat urna tortor vitae lacus.

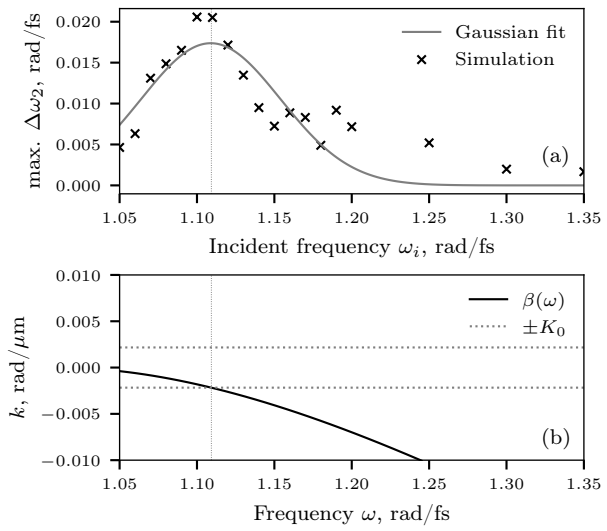

FIG. 7: Resonance behavior of the internal soliton mode during intensive scattering. (a) frequency component oscillation amplitude as a function of incident frequency (b) resonance condition for the internal mode.

Nullam libero mauris, consequat quis, varius et, dictum id, arcu. Mauris mollis tincidunt felis. Aliquam feugiat tellus ut neque. Nulla facilisis, risus a rhoncus fermentum, tellus tellus lacinia purus, et dictum nunc justo sit amet elit.

Aliquam erat volutpat. Nunc eleifend leo vitae magna. In id erat non orci commodo lobortis. Proin neque massa, cursus ut, gravida ut, lobortis eget, lacus. Sed diam. Praesent fermentum tempor tellus. Nullam tempus. Mauris ac felis vel velit tristique imperdiet. Donec at pede. Etiam vel neque nec dui dignissim bibendum. Vivamus id enim. Phasellus neque orci, porta a, aliquet quis, semper a, massa. Phasellus purus. Pellentesque tristique imperdiet tortor. Nam euismod tellus id erat.

Acknowledgements

* Electronic address: oreshnikov.ivan@gmail.com

[1] O. Melchert, S. Willms, S. Bose, A. Yulin, B. Roth, F. Mitschke, U. Morgner, I. Babushkin, and A. Demircan, Physical review letters **123**, 243905 (2019).
[2] N. Akhmediev and M. Karlsson, Physical Review A **51**, 2602 (1995).
[3] V. V. Afanasjev, Y. S. Kivshar, and C. R. Menyuk, Optics letters **21**, 1975 (1996).
[4] R. Driben, A. Yulin, and A. Efimov, Optics express **23**, 19112 (2015).
[5] M. Conforti, S. Trillo, A. Mussot, and A. Kudlinski, Scientific reports **5**, 1 (2015).
[6] L. G. Wright, S. Wabnitz, D. N. Christodoulides, and F. W. Wise, Physical review letters **115**, 223902 (2015).
[7] I. Oreshnikov, R. Driben, and A. Yulin, Physical Review A **96**, 013809 (2017).
[8] S. Amiranashvili and A. Demircan, Physical Review A **82**, 013812 (2010).
[9] G. P. Agrawal (Academic Press, 2013) p. 247.
[10] A. Yulin, D. Skryabin, and P. S. J. Russell, Optics letters **29**, 2411 (2004).
[11] J. M. Dudley and J. R. Taylor, *Supercontinuum generation in optical fibers* (Cambridge University Press, 2010).
[12] A. C. Hindmarsh, Scientific computing , 55 (1983).
[13] P. Virtanen, R. Gommers, T. E. Oliphant, M. Haberland, T. Reddy, D. Cournapeau, E. Burovski, P. Peterson, W. Weckesser, J. Bright, *et al.*, Nature methods **17**, 261 (2020).
[14] `https://github.com/ioreshnikov/two-color-solitons`.
[15] A. Demircan, S. Amiranashvili, and G. Steinmeyer, Physical review letters **106**, 163901 (2011).
[16] L. Tartara, JOSA B **32**, 395 (2015).
[17] I. Oreshnikov, R. Driben, and A. Yulin, Optics letters **40**, 5554 (2015).